Fast Preparation and Detection of a Rydberg Qubit Using Atomic Ensembles

Wenchao Xu,[1] Aditya V. Venkatramani,[2,1] Sergio H. Cantú,[1] Tamara Šumarac,[2,1] Valentin Klüsener,[3,1] Mikhail D. Lukin,[2] and Vladan Vuletić[1]

[1]*Department of Physics and Research Laboratory of Electronics, Massachusetts Institute of Technology, Cambridge, Massachusetts 02139, USA*
[2]*Department of Physics, Harvard University, Cambridge, Massachusetts 02138, USA*
[3]*University of Erlangen-Nuremberg, Erlangen 91054, Germany*

We demonstrate a new approach for fast preparation, manipulation, and collective readout of an atomic Rydberg-state qubit. By making use of Rydberg blockade inside a small atomic ensemble, we prepare a single qubit within 3 μs with a success probability of $F_p = 0.93 \pm 0.02$, rotate it, and read out its state in 6 μs with a single-shot fidelity of $F_d = 0.92 \pm 0.04$. The ensemble-assisted detection is 10^3 times faster than imaging of a single atom with the same optical resolution, and enables fast repeated nondestructive measurement. We observe qubit coherence times of 15 μs, much longer than the π rotation time of 90 ns. Potential applications ranging from faster quantum information processing in atom arrays to efficient implementation of quantum error correction are discussed.

Fast and reliable state initialization and readout of qubits are essential requirements for implementing scalable quantum information systems. Recently, individually controlled highly excited Rydberg atoms have emerged as a promising platform for quantum simulation and computation [1–4]. These systems are enabled by the strong coherent interaction between Rydberg atoms at distances exceeding several micrometers. In combination with the demonstrated ability to deterministically assemble large arrays of individual atoms [5–11], Rydberg-atom arrays have been used to simulate quantum spin models [2] with more than 250 qubits [12–15] to perform multiple-qubit gate operations [16–21], or to create large maximally entangled states [22]. While these quantum simulation and computation systems can operate on microsecond timescales, they could benefit substantially from faster qubit preparation and detection, as both the array preparation process and the optical state readout in most systems require several to many milliseconds [5–7]. Moreover, fast and high-fidelity single-shot qubit readout without atom loss could enable a new generation of experiments with error mitigation, such as quantum error correction and fault tolerant quantum processing [23].

Prior approaches for individual Rydberg-qubit detection include state-dependent ionization and detection of the ions, a relatively fast ($\tau \sim 0.1$ ms) process that has only moderate fidelity [24], and the state-dependent removal of atoms followed by relatively slow ($\tau \sim 10$ ms) fluorescence imaging of the remaining atoms [12,21,25,26] with relatively high fidelities of $F \gtrsim 0.95$. Fast high-intensity fluorescence detection within 20 μs with single-atom resolution has been achieved in Ref. [27]; however, this method as demonstrated is not compatible with atomic arrays, as it does not have the necessary spatial resolution and also requires a large magnetic field. Both ion detection and fluorescence imaging are destructive readout processes, and require a new atomic array to be prepared subsequently, further limiting the cycle time of the quantum processor.

Our detection scheme is based on the proposal by Günter *et al.* [28] to use Rydberg interactions in combination with electromagnetically induced transparency (EIT) [29,30] for collectively enhanced imaging. This method has previously been used to observe Rydberg dynamics [31] without, however, experimentally achieving single-atom resolution. A similar approach has also been used to demonstrate a single-photon switch and a single-photon transistor using Rydberg interactions [32–34].

In this Letter, we demonstrate high-fidelity preparation, manipulation, and detection of a single-Rydberg-atom qubit (and not a collective state as in Refs. [35,36]) inside an atomic ensemble on the microsecond timescale. Starting with $N \sim 400$ trapped ultracold ^{87}Rb atoms, we prepare a qubit between the Rydberg states $|\uparrow\rangle \equiv |r'\rangle = |91P_{3/2}, m_j = 3/2\rangle$ and $|\downarrow\rangle \equiv |r\rangle = |92S_{1/2}, m_j = 1/2\rangle$, perform qubit rotations with a loss of contrast $\delta C \leq 2 \times 10^{-3}$ per 2π pulse, and read out the state optically. Harnessing the collective effect of Rydberg blockade [19], the state preparation and detection are performed in $T_p = 3$ μs and $T_d = 6$ μs with fidelities of $F_p = 0.93 \pm 0.02$ and $F_d = 0.92 \pm 0.04$, respectively. The qubit coherence time of $\tau_c = (15 \pm 5)$ μs, measured with a Ramsey sequence, is much longer than the π rotation time of 90 ns.

Our approach harnesses collective phenomena for speeding up both state preparation and detection. The preparation is accomplished by applying laser and microwave radiation to an ensemble of N atoms, such that any atom can be excited to the Rydberg state, yielding N times faster excitation of the first atom to the Rydberg state than for a single atom, while the preparation of a single excitation is ensured by the Rydberg blockade mechanism [12,37]. Similarly, the signal-to-noise ratio in optical detection is collectively enhanced by a factor $\sim N$: Depending on the state of the single-atom Rydberg qubit, the absorption of probe light by all of the N atoms in the ensemble is simultaneously switched on or off [28].

Our experimental setup is illustrated in Fig. 1(a). A small ensemble with root-mean-square (rms) size of $\sqrt{\langle r^2 \rangle} \approx$ 6 μm containing typically $N \sim 400$ laser-cooled ^{87}Rb atoms is prepared inside a two-beam optical dipole trap with waist sizes $w_1 = 10$ μm and $w_2 = 20$ μm (see Supplemental Material (SM) [38] for details). The trapped atoms are optically pumped into the hyperfine and magnetic sublevel $|g\rangle \equiv |5S_{1/2}, F = 2, m_F = 2\rangle$ that is coupled via a two-photon process involving the transitions $|g\rangle \leftrightarrow |e\rangle \equiv |5P_{3/2}, F = 3, m_F = 3\rangle$ (probe beam Ω_p) and $|e\rangle \leftrightarrow |r\rangle$ (control beam Ω_c) to the Rydberg state $|r\rangle \equiv |92S_{1/2}, m_j = 1/2\rangle$.

To prepare a single atom in the Rydberg state $|r'\rangle$ inside the ensemble, the probe laser and microwave field are detuned by $\Delta_e/(2\pi) = \delta_r/(2\pi) = 100$ MHz from their respective transitions, and in combination with the control field drive a three-photon transition $|g\rangle \leftrightarrow |e\rangle \leftrightarrow |r\rangle \leftrightarrow |r'\rangle$ [see Fig. 1(a)]. By changing the powers of the two optical fields within ~ 3 μs, while keeping the microwave field constant, a process similar to stimulated Raman adiabatic passage (STIRAP) is realized (see SM [38] for details). This process is chosen over direct excitation because it is less sensitive to laser noise and atom number fluctuations. The observed linewidth $\Gamma_3/(2\pi) = 0.6$ MHz of the three-photon transition is much smaller than the energy shift $|\Delta E|/h \gtrsim 10$ MHz at the rms distance $d_0 \equiv \sqrt{2\langle r^2 \rangle} \approx 8$ μm between two atoms in their $|r'\rangle$ state in the ensemble (averaged over angles, see SM [38]). This ensures that excitations of two or more atoms to the Rydberg state are suppressed [12,37]. While the $|r'\rangle$ state has vanishing interactions along certain angular directions (see SM [38]), the admixture of the spherically symmetric $|r\rangle$ state with the microwave field during preparation may help increase the preparation fidelity.

Before discussing how we experimentally verify that only a single Rydberg atom has been prepared, we first describe the detection process. In the following, we associate the Rydberg state $|r'\rangle$ with an effective $|\uparrow\rangle$ state. When the two-photon transition is resonant with the intermediate state [$\Delta_e = 0$, see Fig. 1(a)], the transmitted probe light serves for Rydberg state detection [28] under conditions of EIT [29,30]. If an atom in $|\uparrow\rangle$ is present, the excitation of a Rydberg polariton to the state $|r\rangle$ at a distance R requires an additional interaction energy that in the presence of both van der Waals and exchange interactions is approximately given by $V_{rr'} = C_6/R^6 \pm C_3/R^3$, where $C_6/h = 6310$ GHz μm^6 and $C_3/h = 23.6$ GHz μm^3 (see SM [38]). This interaction energy shifts the EIT resonance and results in a lower transmission of the probe beam for the state $|\uparrow\rangle$.

Figure 2(a) shows the observed photon count histograms of the transmitted light in a 6-μs detection window with and without an atom in $|\uparrow\rangle$. Even in such a short time, the two photon count distributions can be clearly distinguished. The time-resolved average count rate [Fig. 2(b)] reveals that the transmission $T_{|\uparrow\rangle}$ for $|\uparrow\rangle$ increases with time, whereas the high transmission without an atom in $|\uparrow\rangle$ is almost constant, and decreases only slowly. The latter may be explained by a decay of the slow-light $|r\rangle$ polaritons to other Rydberg states, producing randomly a stationary atom in some Rydberg state, that then blocks the EIT transmission. The increase in the average transmission $T_{|\uparrow\rangle}$, on the other hand, can be explained by a light-induced loss process of the Rydberg atom in $|\uparrow\rangle$ during detection, which
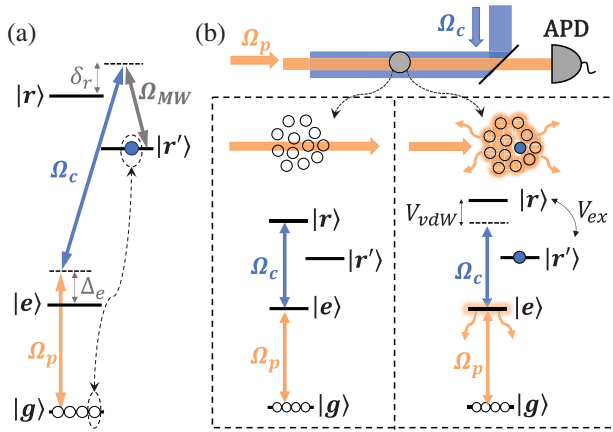

FIG. 1. Fast collective detector of a single Rydberg atom. (a) State initialization. An atom is prepared in the Rydberg state $|r'\rangle$ through a three-photon process involving the preparation beam (Ω_p, orange), the control beam (Ω_c, blue), and a microwave field (Ω_{MW}, grey). The detunings from the two intermediate states are $\Delta_e = \delta_r = 2\pi \times 100$ MHz. The preparation of a single atom in $|r'\rangle$ is ensured by the strong interaction between two atoms in $|r'\rangle$ [1]. (b) A probe field (orange, waist size $w_p = 4.5$ μm) in combination with the control field ($w_c = 12.5$ μm) couples atoms to the Rydberg state $|r\rangle$. Under conditions of EIT ($\Delta_e = \delta_r = 0$), high transmission through the atomic medium results in a large number of detected photons (left). On the other hand, if the Rydberg state $|r'\rangle$ is populated by an atom (right), then the strong interaction between $|r\rangle$ and $|r'\rangle$ removes the EIT condition, resulting in a significant reduction of transmitted photon number due to absorption by the ensemble. The interaction $V_{rr'}$ contains both dipolar-exchange (V_{ex}) and van der Waals components (V_{vdW}) (see SM).
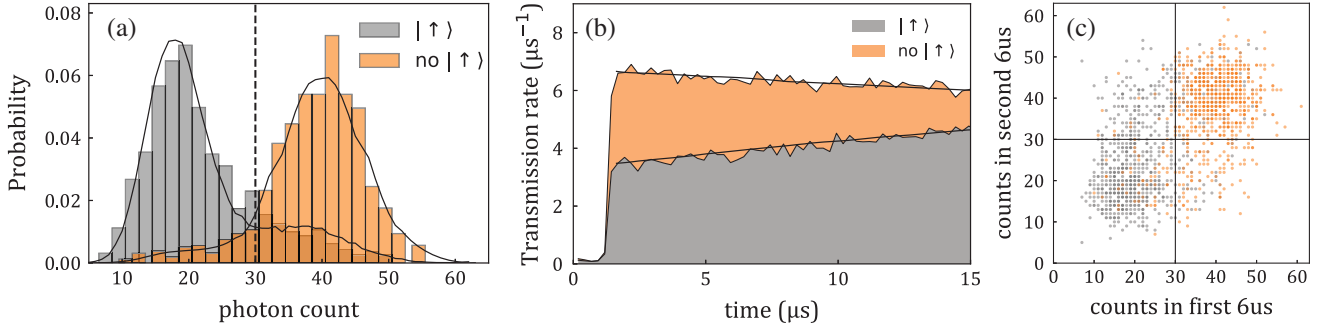
FIG. 2. (a) Histogram of the transmitted probe photon number for state detection performed in 6 μs. Grey and orange histograms correspond to the presence and absence of an atom in Rydberg state $|r'\rangle \equiv |\uparrow\rangle$, respectively. The solid lines in (a), (b) indicate a theoretical model that for the presence (absence) of an atom in $|\uparrow\rangle$ assumes random sudden loss of the Rydberg atom in $|\uparrow\rangle$ (sudden decay of the slow-light polariton into a Rydberg state) at a rate 0.035 μs^{-1} (0.015 μs^{-1}). The dashed line indicates the detection threshold that gives us the highest fidelity of differentiating two distributions. The control Rabi frequency is $\Omega_c/(2\pi) = 25$ MHz, and the probabilities for collecting and detecting a transmitted probe photon are 0.90 and 0.47, respectively. (b) Time-resolved photon count rate during detection. (c) Correlation plot of number of detected-photon counts in two consecutive 6 μs measurements in the same run of the experiment. Gray (orange) points represent transmission data when we prepare (do not prepare) the $|\uparrow\rangle$ state. Vertical and horizontal lines represent threshold counts for state discrimination.

leads to a sudden increase in transmission at a random time. The observed signal reduction is primarily associated with the control light, and is too fast to be explained by photoionization [43,46] or the repulsive ac-Stark shift (see SM [38] for details). We hypothesize that a small residual electric field of a few 10 mV/cm mixes a $|92S\rangle$ component into the $|91P\rangle$ state, so that the control light can couple the $|\uparrow\rangle$ state, which contains a small component of $|92S\rangle$ in it, to the rapidly decaying $|e\rangle$ state, causing a sudden loss of the atom in $|\uparrow\rangle$.

Modeling the system as a removal of blockade at a random time yields excellent agreement with the photon count histograms observed at different detection times (see SM [38]). From this we infer a preparation fidelity for the state $|\uparrow\rangle$ (i.e., an atom in $|r'\rangle$) of $F_p = 0.93 \pm 0.02$ (see SM [38] for details). The detection fidelity (probability of correctly identifying the underlying state $|\uparrow\rangle$) after removing the state preparation error is then $F_d = 0.92 \pm 0.04$.

Figure 2(c) demonstrates that we can perform repeated ("nondestructive") measurements on the system, where a second 6-μs measurement yields good agreement with the first measurement: The average conditional probability for the second measurement to have the same outcome as the first measurement is $p = 0.79 \pm 0.03$ (see SM [38] for details). The detection system can also be viewed as a single-atom transistor for light. We then achieve a gain of $G = 17 \pm 1$ in 6 μs, somewhat larger than the gain of $G = 10$ in 30 μs achieved in the Rydberg system of Ref. [33].

We implement a qubit in our system by defining the state with a single atom in $|r\rangle$ as the $|\downarrow\rangle$ state. Coherent rotations in the $\{|\uparrow\rangle, |\downarrow\rangle\}$ manifold are induced by applying the microwave field. After a qubit rotation, we detect the resulting state by turning on the coupling light slightly (1 μs) earlier than the probe light, such that the state $|r\rangle$ is quickly deexcited by the strong coupling laser to the

unstable state $|e\rangle$, which decays by photon emission in 30 ns (see Fig. 1). Thus, as far as the detection process is concerned, the state $|\downarrow\rangle$ (atom in $|r\rangle$) is equivalent to having no Rydberg excitation at all, while the state $|\uparrow\rangle$ (atom in $|r'\rangle$) remains unaffected by the detection light, and leads to Rydberg blockade of the probe transmission. If the photon count is above or below a chosen detection threshold [see Fig. 2(a)], we identify the qubit state as $|\downarrow\rangle$ or $|\uparrow\rangle$, respectively.

Figure 3 shows Rabi oscillations with the full sequence of state preparation, qubit rotation, and detection. The trap light is turned off during the sequence to avoid light shifts of the states. We use two microwave antennas with adjusted relative phase and amplitude to suppress the π polarization component of the microwave field that can couple atoms in $|\downarrow\rangle$ to the magnetic sublevel $m_j = 1/2$ in the $91P_{3/2}$
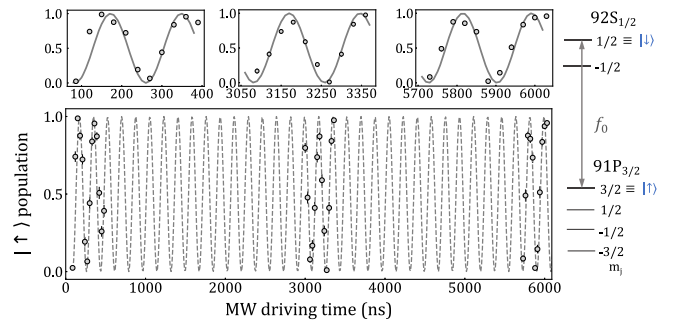

FIG. 3. A microwave field at a frequency $f_0 = 4814.2$ MHz is applied to drive Rabi oscillations between $|\uparrow\rangle$ and $|\downarrow\rangle$ at an oscillation frequency $\Omega/(2\pi) = 5.3$ MHz. Each point is an average of ~150 repetitions. The error bars are the standard deviation of the mean. The fitted contrast loss per 2π pulse is $\delta C < 2 \times 10^{-3}$. The relevant energy level diagrams are shown on the right.

manifold, offset by 17 MHz in an applied magnetic field of 9 G. The remaining coupling to other magnetic sublevels limits the maximum Rabi frequency on the $|\uparrow\rangle \leftrightarrow |\downarrow\rangle$ transition to $\lesssim 5$ MHz. The Rabi oscillations show no observable damping on the 6 μs timescale, corresponding to a contrast loss per 2π pulse of $\delta C \leq 2 \times 10^{-3}$.

The observed contrast of the Rabi oscillations can be used to determine the probability that two excitations in $|r'\rangle$ were simultaneously created in the ensemble. Because of the large interaction energy between two atoms in $|r'\rangle$ and $|r\rangle$, the Rabi oscillations with two excitations would very quickly wash out on a timescale $h/V_{rr'}(d_0) \sim 40$ ns. From the observed contrast of the Rabi oscillation we conclude that the probability for preparing two excitations is below 1%.

We use a Ramsey measurement to characterize the coherence time of the Rydberg qubit embedded inside the atomic cloud. Two $\pi/2$ pulses are applied with a temporal separation τ between them, and their relative phase is scanned to obtain a Ramsey fringe at given τ. Figure 4 displays the contrast of the Ramsey fringes as a function of Ramsey time τ. By fitting the contrast to a Gaussian decay function, we obtain the e^{-2} dephasing time as (15 ± 5) μs. Possible dephasing mechanisms include electric-field fluctuations acting on the highly polarizable Rydberg states, magnetic field fluctuations, and interactions between the Rydberg atom and the surrounding ground state atoms [47]. We also note that neither the Rabi flopping nor the Ramsey measurement depend on whether we have encoded the qubit in a single atom or collectively in a W state [35]. However, previous measurements involving storage and retrieval of photons indicate that the collective state decoheres during preparation, such that the qubit is ultimately encoded in a single atom [48].
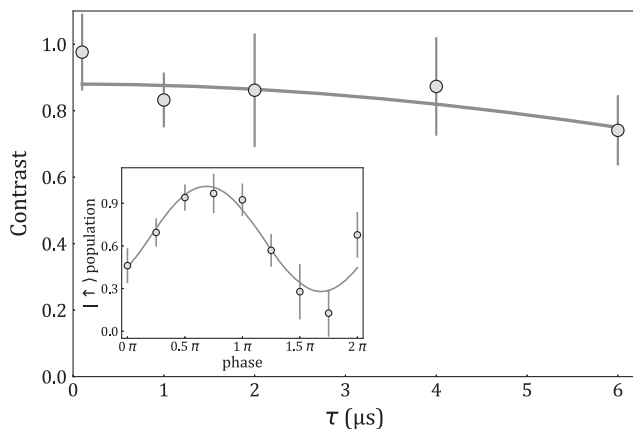

FIG. 4. Ramsey measurements consisting of two $\pi/2$ pulses separated by a time τ. The phase of the second $\pi/2$ pulse is scanned to obtain a Ramsey fringe. The contrast of the Ramsey fringe is plotted as a function of τ. The solid curve is a fit to a Gaussian decay function $Ae^{-(\tau/T_2^*)^2}$, yielding a dephasing time $T_2^* = (15 \pm 5)$ μs and $A = 0.88 \pm 0.04$. Inset: Ramsey fringe at $\tau = 1000$ ns.

In summary, by harnessing collective effects in a small atomic ensemble, we have demonstrated a method for the rapid preparation and detection of a Rydberg qubit. The preparation and detection fidelities demonstrated in this work can likely be further increased in the future. The preparation fidelity for a single excitation can be improved by modifying the preparation sequence (see SM [38]) or using smaller ensemble size, since such ensembles would provide even higher energy cost for multiple excitation. The size of the ensemble cannot, however, be made arbitrarily small, since at higher atomic densities, necessary to maintain the same optical depth OD ~ 1, Rydberg molecule formation [49] could lead to loss. Given our current average atomic density of $\langle n \rangle = 2 \times 10^{11}$ cm^{-3}, reducing the ensemble size by a factor of 2 should be possible, which would likely reduce the preparation error by more than an order of magnitude.

Our demonstrated detection fidelity, on the other hand, is limited by the loss of the Rydberg atom prepared in the $|r'\rangle$ state. This loss is mainly caused by the control light in the detection stage, and thus could be mitigated by using two ensembles, one for hosting the qubit and the other for detection, located within a blockade radius from each other. Assuming a measurement time of 10 μs, this configuration could allow for a nondestructive, fast qubit readout with detection fidelity over 99%, a crucial tool necessary for implementing quantum error correction [23]. In addition, such a readout can also enable studies of quantum feedback [50], quantum Zeno effect [51], quantum jumps [52], and can act as a fast probe of Rydberg super-atom dynamics [53].

The detection scheme can be readily implemented in different Rydberg platforms [2,7,13], where a single atom would be replaced by a small ensemble, as demonstrated in Ref. [54]. Alternatively, one can place a small ensemble within the Rydberg blockade radius of each single atom for fast detection, or even within the blockade radius of several single atoms for fast parity measurements, and possibly even error correction. To suppress diffusion of the Rydberg atom between different ensembles due to the exchange interaction during detection, it may be necessary to adjust the lattice constant of the array or the principal quantum numbers of the Rydberg states used.

W. X., A. V. V., and S. H. C. contributed equally to this work.

[1] M. D. Lukin, M. Fleischhauer, R. Cote, L. M. Duan, D. Jaksch, J. I. Cirac, and P. Zoller, Dipole Blockade and

Quantum Information Processing in Mesoscopic Atomic Ensembles, Phys. Rev. Lett. **87**, 037901 (2001).

[2] A. Browaeys and T. Lahaye, Many-body physics with individually controlled rydberg atoms, Nat. Phys. **16**, 132 (2020).

[3] M. Saffman, Quantum computing with atomic qubits and rydberg interactions: progress and challenges, J. Phys. B **49**, 202001 (2016).

[4] M. Morgado and S. Whitlock, Quantum simulation and computing with Rydberg-interacting qubits, AVS Quantum Sci. **3**, 023501 (2021).

[5] M. Endres, H. Bernien, A. Keesling, H. Levine, E. R. Anschuetz, A. Krajenbrink, C. Senko, V. Vuletic, M. Greiner, and M. D. Lukin, Atom-by-atom assembly of defect-free one-dimensional cold atom arrays, Science **354**, 1024 (2016).

[6] D. Barredo, S. De Léséleuc, V. Lienhard, T. Lahaye, and A. Browaeys, An atom-by-atom assembler of defect-free arbitrary two-dimensional atomic arrays, Science **354**, 1021 (2016).

[7] D. Barredo, V. Lienhard, S. De Leseleuc, T. Lahaye, and A. Browaeys, Synthetic three-dimensional atomic structures assembled atom by atom, Nature (London) **561**, 79 (2018).

[8] A. Kumar, T.-Y. Wu, F. Giraldo, and D. S. Weiss, Sorting ultracold atoms in a three-dimensional optical lattice in a realization of maxwell's demon, Nature (London) **561**, 83 (2018).

[9] D. O. de Mello, D. Schäffner, J. Werkmann, T. Preuschoff, L. Kohfahl, M. Schlosser, and G. Birkl, Defect-Free Assembly of 2d Clusters of More Than 100 Single-Atom Quantum Systems, Phys. Rev. Lett. **122**, 203601 (2019).

[10] M. O. Brown, T. Thiele, C. Kiehl, T.-W. Hsu, and C. A. Regal, Gray-Molasses Optical-Tweezer Loading: Controlling Collisions for Scaling Atom-Array Assembly, Phys. Rev. X **9**, 011057 (2019).

[11] H. Kim, W. Lee, H.-G. Lee, H. Jo, Y. Song, and J. Ahn, In situ single-atom array synthesis using dynamic holographic optical tweezers, Nat. Commun. **7**, 1 (2016).

[12] H. Bernien, S. Schwartz, A. Keesling, H. Levine, A. Omran, H. Pichler, S. Choi, A. S. Zibrov, M. Endres, M. Greiner et al., Probing many-body dynamics on a 51-atom quantum simulator, Nature (London) **551**, 579 (2017).

[13] A. Keesling, A. Omran, H. Levine, H. Bernien, H. Pichler, S. Choi, R. Samajdar, S. Schwartz, P. Silvi, S. Sachdev et al., Quantum kibble–zurek mechanism and critical dynamics on a programmable rydberg simulator, Nature (London) **568**, 207 (2019).

[14] S. Ebadi, T. T. Wang, H. Levine, A. Keesling, G. Semeghini, A. Omran, D. Bluvstein, R. Samajdar, H. Pichler, W. W. Ho, S. Choi, S. Sachdev, M. Greiner, V. Vuletic, and M. D. Lukin, Quantum phases of matter on a 256-atom programmable quantum simulator, arXiv:2012.12281.

[15] P. Scholl, M. Schuler, H. J. Williams, A. A. Eberharter, D. Barredo, K.-N. Schymik, V. Lienhard, L.-P. Henry, T. C. Lang, T. Lahaye, A. M. Läuchli, and A. Browaeys, Programmable quantum simulation of 2d antiferromagnets with hundreds of rydberg atoms, arXiv:2012.12268.

[16] L. Isenhower, E. Urban, X. L. Zhang, A. Gill, T. Henage, T. A. Johnson, T. G. Walker, and M. Saffman, Demonstration of a Neutral Atom Controlled-Not Quantum Gate, Phys. Rev. Lett. **104**, 010503 (2010).

[17] T. M. Graham, M. Kwon, B. Grinkemeyer, Z. Marra, X. Jiang, M. T. Lichtman, Y. Sun, M. Ebert, and M. Saffman, Rydberg-Mediated Entanglement in a Two-Dimensional Neutral Atom Qubit Array, Phys. Rev. Lett. **123**, 230501 (2019).

[18] H. Levine, A. Keesling, G. Semeghini, A. Omran, T. T. Wang, S. Ebadi, H. Bernien, M. Greiner, V. Vuletić, H. Pichler et al., Parallel Implementation of High-Fidelity Multiqubit Gates with Neutral Atoms, Phys. Rev. Lett. **123**, 170503 (2019).

[19] D. Jaksch, J. I. Cirac, P. Zoller, S. L. Rolston, R. Côté, and M. D. Lukin, Fast Quantum Gates for Neutral Atoms, Phys. Rev. Lett. **85**, 2208 (2000).

[20] H. Levine, A. Keesling, A. Omran, H. Bernien, S. Schwartz, A. S. Zibrov, M. Endres, M. Greiner, V. Vuletić, and M. D. Lukin, High-Fidelity Control and Entanglement of Rydberg-Atom Qubits, Phys. Rev. Lett. **121**, 123603 (2018).

[21] I. S. Madjarov, J. P. Covey, A. L. Shaw, J. Choi, A. Kale, A. Cooper, H. Pichler, V. Schkolnik, J. R. Williams, and M. Endres, High-fidelity control, detection, and entanglement of alkaline-earth rydberg atoms, Nat. Phys. **16**, 857 (2020).

[22] A. Omran, H. Levine, A. Keesling, G. Semeghini, T. T. Wang, S. Ebadi, H. Bernien, A. S. Zibrov, H. Pichler, S. Choi et al., Generation and manipulation of schrödinger cat states in rydberg atom arrays, Science **365**, 570 (2019).

[23] S. J. Devitt, W. J. Munro, and K. Nemoto, Quantum error correction for beginners, Rep. Prog. Phys. **76**, 076001 (2013).

[24] T. F. Gallagher, Rydberg Atoms (Cambridge University Press, Cambridge, England, 2005), Vol. 3.

[25] A. Gaëtan, Y. Miroshnychenko, T. Wilk, A. Chotia, M. Viteau, D. Comparat, P. Pillet, A. Browaeys, and P. Grangier, Observation of collective excitation of two individual atoms in the rydberg blockade regime, Nat. Phys. **5**, 115 (2009).

[26] A. Fuhrmanek, Y. R. P. Sortais, P. Grangier, and A. Browaeys, Measurement of the atom number distribution in an optical tweezer using single-photon counting, Phys. Rev. A **82**, 023623 (2010).

[27] A. Bergschneider, V. M. Klinkhamer, J. H. Becher, R. Klemt, G. Zürn, P. M. Preiss, and S. Jochim, Spin-resolved single-atom imaging of ^{6}Li in free space, Phys. Rev. A **97**, 063613 (2018).

[28] G. Günter, M. Robert-de Saint-Vincent, H. Schempp, C. S. Hofmann, S. Whitlock, and M. Weidemüller, Interaction Enhanced Imaging of Individual Rydberg Atoms in Dense Gases, Phys. Rev. Lett. **108**, 013002 (2012).

[29] M. Fleischhauer, A. Imamoglu, and J. P. Marangos, Electromagnetically induced transparency: Optics in coherent media, Rev. Mod. Phys. **77**, 633 (2005).

[30] A. K. Mohapatra, T. R. Jackson, and C. S. Adams, Coherent Optical Detection of Highly Excited Rydberg States using Electromagnetically Induced Transparency, Phys. Rev. Lett. **98**, 113003 (2007).

[31] G. Günter, H. Schempp, M. Robert-de Saint-Vincent, V. Gavryusev, S. Helmrich, C. Hofmann, S. Whitlock, and M. Weidemüller, Observing the dynamics of dipole-mediated

energy transport by interaction-enhanced imaging, Science **342,** 954 (2013).

[32] S. Baur, D. Tiarks, G. Rempe, and S. Dürr, Single-Photon Switch Based on Rydberg Blockade, Phys. Rev. Lett. **112,** 073901 (2014).

[33] H. Gorniaczyk, C. Tresp, J. Schmidt, H. Fedder, and S. Hofferberth, Single-Photon Transistor Mediated by Interstate Rydberg Interactions, Phys. Rev. Lett. **113,** 053601 (2014).

[34] D. Tiarks, S. Baur, K. Schneider, S. Dürr, and G. Rempe, Single-Photon Transistor using a Förster Resonance, Phys. Rev. Lett. **113,** 053602 (2014).

[35] M. Ebert, M. Kwon, T. G. Walker, and M. Saffman, Coherence and Rydberg Blockade of Atomic Ensemble Qubits, Phys. Rev. Lett. **115,** 093601 (2015).

[36] N. L. Spong, Y. Jiao, O. D. Hughes, K. J. Weatherill, I. Lesanovsky, and C. S. Adams, The Robustness of a Collectively Encoded Rydberg Qubit, arXiv:2010.11794 [Phys. Rev. Lett. (to be published)].

[37] E. Urban, T. A. Johnson, T. Henage, L. Isenhower, D. Yavuz, T. Walker, and M. Saffman, Observation of rydberg blockade between two atoms, Nat. Phys. **5,** 110 (2009).

[38] See Supplemental Material at http://link.aps.org/supplemental/10.1103/PhysRevLett.127.050501 for details on experimental setup and analysis, which includes reference [39–45].

[39] F. Robicheaux, Ionization due to the interaction between two Rydberg atoms, J. Phys. B **38,** S333 (2005).

[40] W. Li, P. J. Tanner, and T. F. Gallagher, Dipole-Dipole Excitation and Ionization in an Ultracold Gas of Rydberg Atoms, Phys. Rev. Lett. **94,** 173001 (2005).

[41] M. Kiffner, D. Ceresoli, W. Li, and D. Jaksch, Quantum mechanical calculation of Rydberg–Rydberg autoionization rates, J. Phys. B **49,** 204004 (2016).

[42] M. Mizoguchi, Y. Zhang, M. Kunimi, A. Tanaka, S. Takeda, N. Takei, V. Bharti, K. Koyasu, T. Kishimoto, D. Jaksch *et al.*, Ultrafast Creation of Overlapping Rydberg Electrons in an Atomic BEC and Mott-Insulator Lattice, Phys. Rev. Lett. **124,** 253201 (2020).

[43] M. Saffman and T. G. Walker, Analysis of a quantum logic device based on dipole-dipole interactions of optically trapped Rydberg atoms, Phys. Rev. A **72,** 022347 (2005).

[44] P. Neumann, J. Beck, M. Steiner, F. Rempp, H. Fedder, P. R. Hemmer, J. Wrachtrup, and F. Jelezko, Single-shot readout of a single nuclear spin, Science **329,** 542 (2010).

[45] V. B. Braginsky and F. Y. Khalili, Quantum nondemolition measurements: the route from toys to tools, Rev. Mod. Phys. **68,** 1 (1996).

[46] S. E. Anderson and G. Raithel, Ionization of rydberg atoms by standing-wave light fields, Nat. Commun. **4,** 1 (2013).

[47] M. Schlagmüller, T. C. Liebisch, F. Engel, K. S. Kleinbach, F. Böttcher, U. Hermann, K. M. Westphal, A. Gaj, R. Löw, S. Hofferberth, T. Pfau, J. Pérez-Ríos, and C. H. Greene, Ultracold Chemical Reactions of a Single Rydberg Atom in a Dense Gas, Phys. Rev. X **6,** 031020 (2016).

[48] T. Peyronel, O. Firstenberg, Q.-Y. Liang, S. Hofferberth, A. V. Gorshkov, T. Pohl, M. D. Lukin, and V. Vuletić, Quantum nonlinear optics with single photons enabled by strongly interacting atoms, Nature (London) **488,** 57 (2012).

[49] V. Bendkowsky, B. Butscher, J. Nipper, J. P. Shaffer, R. Löw, and T. Pfau, Observation of ultralong-range rydberg molecules, Nature (London) **458,** 1005 (2009).

[50] C. Sayrin, I. Dotsenko, X. Zhou, B. Peaudecerf, T. Rybarczyk, S. Gleyzes, P. Rouchon, M. Mirrahimi, H. Amini, M. Brune *et al.*, Real-time quantum feedback prepares and stabilizes photon number states, Nature (London) **477,** 73 (2011).

[51] G. Barontini, L. Hohmann, F. Haas, J. Estève, and J. Reichel, Deterministic generation of multiparticle entanglement by quantum zeno dynamics, Science **349,** 1317 (2015).

[52] Z. Minev, S. Mundhada, S. Shankar, P. Reinhold, R. Gutiérrez-Jáuregui, R. Schoelkopf, M. Mirrahimi, H. Carmichael, and M. Devoret, To catch and reverse a quantum jump mid-flight, Nature (London) **570,** 200 (2019).

[53] J. Zeiher, P. Schauß, S. Hild, T. Macrì, I. Bloch, and C. Gross, Microscopic Characterization of Scalable Coherent Rydberg Superatoms, Phys. Rev. X **5,** 031015 (2015).

[54] Y. Wang, S. Shevate, T. Wintermantel, M. Morgado, G. Lochead, and S. Whitlock, Preparation of hundreds of microscopic atomic ensembles in optical tweezer arrays, New J. Phys. **6,** 54 (2020).